

A figure-of-merit-based framework to evaluate photovoltaic materials

Andrea Crovetto^{1,*}

¹*National Centre for Nano Fabrication and Characterization (DTU Nanolab),
Technical University of Denmark, 2800 Kongens Lyngby, Denmark*

I propose a general quantitative framework to evaluate the quality, track the historical development, and guide future optimization of photovoltaic (PV) absorbers at any development level, including both experimentally synthesized and computer-simulated materials. The framework is based on a PV figure of merit designed to include efficiency limitations due to imperfect photo-carrier collection that are not included in classic detailed balance methods. Figure-of-merit-driven efficiency limits including collection losses are calculated for 28 experimentally synthesized PV absorbers and 9 PV absorbers simulated by electronic structure methods. Among emerging absorbers for which no working solar cells have yet been reported, there are very large differences in their likelihood to achieve high PV efficiencies.

The pace of exploration of new photovoltaic (PV) absorber materials has accelerated in recent years, owing in part to the popularization of high-throughput materials research methods and the desire to find new absorbers with similar performance and process tolerance to halide perovskites but without their stability and toxicity drawbacks. Various problems in emerging PV materials research are still largely unresolved, specifically: (i) quantifying the efficiency potential of new absorbers during their early development stage, (ii) guiding their optimization, and (iii) helping researchers make rational decisions on which materials are worth investigating.

These problems are fundamentally linked to the methods available to estimate the maximum PV efficiency of semiconducting absorbers. The physical principle of detailed balance between photon absorption and emission is the cornerstone of the most influential efficiency limits, which consist of the classic Shockley-Queisser (SQ) limit [2, 3] and subsequent extensions to include the effect of non-radiative recombination. [4–7] Even though these methods are powerful predictors of open-circuit voltage limits in solar cells, they do not consider efficiency limitations arising from imperfect carrier collection, which often occurs under various combinations of carrier mobilities, doping density, and dielectric constant. [8, 9] Carrier collection losses affect short circuit current densities and fill factors but are difficult to model in a unified manner. [5, 8, 9] Thus, detailed-balance methods provide upper bounds to the maximum efficiency achievable by a real PV absorber.

To address this problem, here I propose an alternative route to the definition of efficiency limits. Rather than deducing them from fundamental physics (as in detailed balance methods), I suggest a phenomenological efficiency limit by an inductive methodology based on the recently developed Γ_{PV} photovoltaic figure of merit (FOM). [1] The Γ_{PV} FOM provides a general quantitative framework to evaluate the quality, track the historical development, and guide future optimization of a generic PV

absorber at any development level.

The Γ_{PV} FOM is a unitless function of eight properties of the PV absorber's bulk:

$$\Gamma_{\text{PV}} = f(\alpha, \sigma, \tau, \mu, n, \epsilon, m, E_g) \quad (1)$$

Here, α and σ are parameters describing the spectral average and spectral dispersion of the absorption coefficient spectrum, τ is the non-radiative recombination lifetime, μ is the carrier mobility, n is the doping density, ϵ is the static dielectric constant, m is the density-of-states (DOS) effective mass, and E_g is the band gap. Definitions of these properties are given in Ref. [1], including potential strategies to deal with direction- and carrier-type dependence.

The Γ_{PV} FOM is defined as:

$$\Gamma_{\text{PV}} = E_g^{2.5} \left(\frac{\mathcal{A}_1 \mathcal{A}_2 \mathcal{D}_1}{\mathcal{D}_2 \mathcal{D}_3 \mathcal{D}_4 (1 + \mathcal{T}_1 \mathcal{T}_2 \mathcal{T}_3) (1 + \mathcal{S}_1 \mathcal{S}_2)} \right)^{E_g^{-0.8}} \quad (2)$$

The various factors $\mathcal{A}_1, \mathcal{A}_2, \mathcal{D}_1 \dots \mathcal{S}_2$ in Eq. 2 are expressions [1] containing the eight properties listed in Eq. 1.

The value of Γ_{PV} can be calculated for any candidate PV absorber at any development level, as long as the eight bulk properties in Eq. 1 have been measured, calculated, or estimated. Once Γ_{PV} has been determined for a certain absorber, the maximum PV efficiency achievable by that absorber in a planar single-junction solar cell under the the standard 1-Sun, AM1.5G spectrum can be estimated as η_{Γ} , defined as:

$$\eta_{\Gamma}(\Gamma_{\text{PV}}, \eta_{\text{sq}}) = \frac{\eta_{\text{sq}}}{\left(1 + \frac{k_1 \Gamma_{\text{PV}}^{-0.235}}{1 + k_2 \Gamma_{\text{PV}}^{0.869}} \right) (1 + k_3 \Gamma_{\text{PV}}^{-0.362})} \quad (3)$$

Here, η_{sq} is the Shockley-Queisser limiting efficiency of the absorber, which is readily calculated from E_g , [2] and k_1, k_2, k_3 are fixed parameters. [1] For easier comparison between different PV absorbers with different band gaps,

* E-mail: ancro@dtu.dk

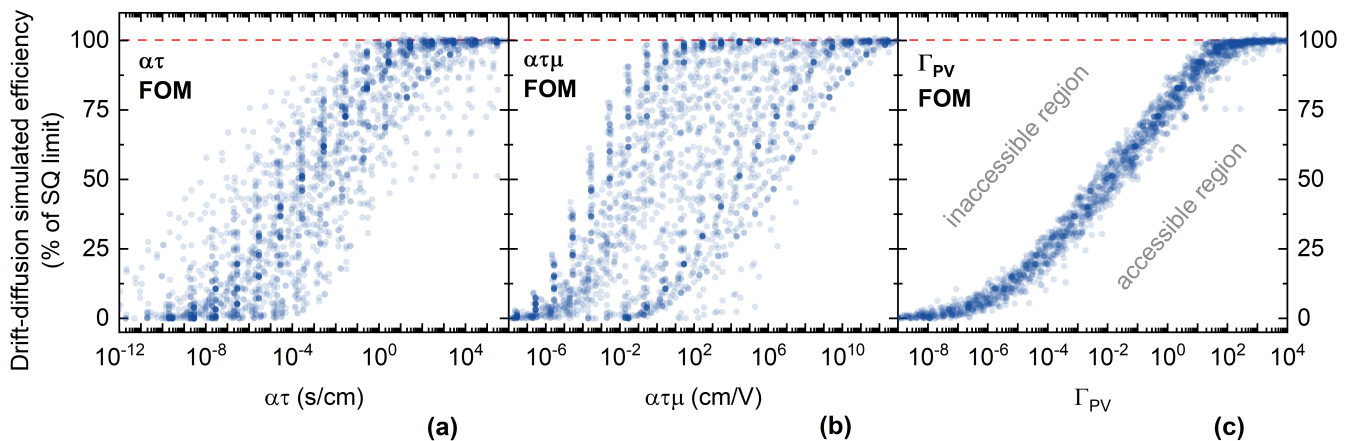


FIG. 1. Predictive ability of the $\alpha\tau$ (a), $\alpha\tau\mu$ (b), and Γ_{PV} figures of merit (c). The maximum efficiency of over 2500 hypothetical absorbers with different combinations of the α , σ , τ , μ , n , ϵ , m , and E_g properties (as obtained by drift-diffusion simulation) is plotted against the three FOMs. These data points constituted a training set in the original development of the Γ_{PV} FOM. [1] Efficiencies are expressed as fraction of the SQ limit, indicated by a red dashed line. The Γ_{PV} FOM splits the efficiency versus FOM space into an accessible and an inaccessible region.

η_Γ will often be expressed as a fraction of the Shockley-Queisser limit. This SQ-normalized efficiency is defined as $\eta_{\Gamma, sq} = \eta_\Gamma / \eta_{sq}$.

The predictive capability of Γ_{PV} is shown in Fig. 1 and compared to the case of the simpler $\alpha\tau$ and $\alpha\tau\mu$ FOMs. [10] The three plots in Fig. 1 show the maximum SQ-normalized efficiency of over 2500 hypothetical absorbers (as obtained by explicit drift-diffusion simulation) versus the three FOMs calculated for the same absorbers. In the simulation [1] the only PV losses besides radiative recombination are due to non-optimal values of the eight bulk properties used to define Γ_{PV} (Eq. 1). It is apparent that the $\alpha\tau$ and $\alpha\tau\mu$ FOMs are generally not predictive of efficiency, although they are useful indicators under certain conditions. [1, 10] On the other hand, the Γ_{PV} FOM seems to have higher predictive power because the simulated data roughly follows a single function that approaches zero for low Γ_{PV} values and η_{sq} for high Γ_{PV} values (Fig. 1(c)). This function is just the SQ-normalized version of the η_Γ function defined in Eq. 3 and it is shown in Fig. 2 as a black line.

The Γ_{PV} FOM naturally leads to the definition of an "accessible region" (below the $\eta_{\Gamma, sq}$ curve in Fig. 2) which is the efficiency range that PV absorbers can realistically access as a function of their figure of merit. The "inaccessible region" above the $\eta_{\Gamma, sq}$ curve would be allowed by the SQ limit alone, but is not allowed by the additional losses introduced by non-optimal values of the eight bulk properties. The error bar of the $\eta_{\Gamma, sq}$ efficiency limit is $\pm 3.4\%$ absolute, [1] under the assumption that the values of α , σ , τ , μ , n , ϵ , m , and E_g used to calculate Γ_{PV} are known exactly. This corresponds to an absolute error around $\pm 1.1\%$ on the actual η_Γ efficiency (not SQ-normalized) for PV absorbers in the 1.1 eV to 1.5 eV band gap range, and less for absorbers outside this range.

In Fig. 2, the maximum (SQ-normalized) experimen-

tal efficiency $\eta_{exp, sq}$ demonstrated by 28 emerging and established PV absorbers in a planar solar cell configuration is plotted as a function of their corresponding Γ_{PV} FOM. As expected, all absorbers lie in the accessible region defined by the Γ_{PV} FOM. Several absorbers lie within error bar of the $\eta_{\Gamma, sq}$ limit, indicating that solar cell architectures, contact layers, and interfaces are sufficiently optimized and do not introduce significant losses at the current level of bulk material quality in these absorbers. GaAs is the absorber with both the highest FOM (20) and the maximum SQ-normalized experimental efficiency (88%). Alloyed perovskites based on $CH_5N_2PbI_3$ (triple-cation and double-anion) have the second highest FOM, followed by c-Si and $CH_3NH_3PbI_3$ perovskites (MAPbI₃). Since the efficiency of c-Si cells is limited by Auger recombination due to particularly weak absorption in Si, [11] there is very limited scope for efficiency increase by improvement of bulk material properties in c-Si (Fig. 2), except for increase in α , which would make c-Si cells less limited by Auger recombination. Multicrystalline silicon (mc-Si), Cu(In,Ga)Se₂ (CIGSe), and CdSeTe have similar FOMs (0.5 to 1) and SQ-normalized record efficiencies (around 70%).

According to the FOM analysis, further efficiency increases in GaAs, c-Si, mc-Si, and CIGSe cells are unlikely unless their bulk properties are improved. On the other hand, higher efficiencies in CdSeTe and perovskite solar cells are not prohibited by their current material quality, so device and interface optimization may be a promising path towards improved solar cell performance. In fact, the Γ_{PV} FOM suggests that it may already be possible for state-of-the-art perovskite alloys to surpass the efficiency of GaAs solar cells without further work on their bulk properties.

Many PV absorbers fall in the intermediate 0.003 to 0.3 Γ_{PV} range (Fig. 2), but none of them lie within

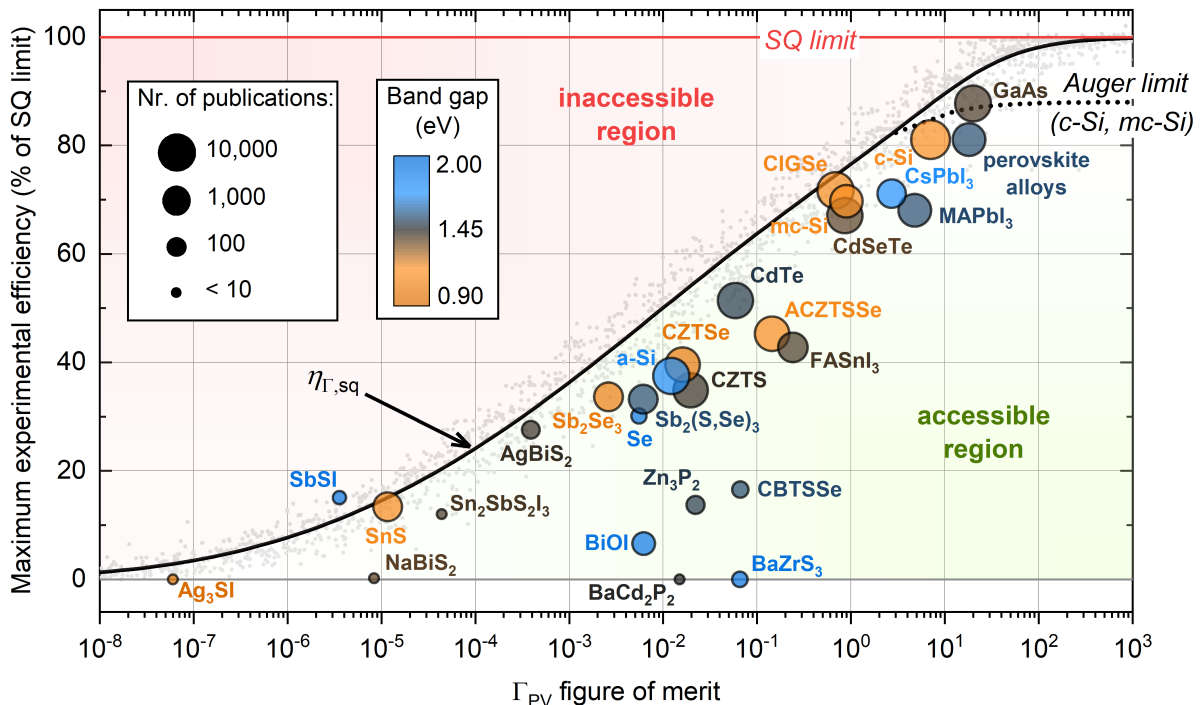


FIG. 2. Performance status of 28 experimentally synthesized PV absorbers, expressed as record efficiency (y-axis, normalized to their SQ limit) versus Γ_{PV} FOM (x-axis). Record solar cells for all materials except SbSI have a planar architecture. The thick black line is the $\eta_{\Gamma,sq}$ efficiency limit (Eq. 3). The dotted line indicates the Auger limit for c-Si and mc-Si (more stringent than their SQ limit). In this representation, the SQ limit is always 100%. The size of the data points is proportional to the logarithm of the number of publications referring to each absorber in a PV context. The color of the data points indicates the band gap of each absorber. The small light grey data points are the training set used to derive the Γ_{PV} FOM (identical to the data points in Fig. 1(c)). They give a visual impression of the $\pm 3.4\%$ absolute error bar of $\eta_{\Gamma,sq}$ as an estimator of efficiency limits. The material properties used to calculate Γ_{PV} for each absorber are listed in Table I, Supporting Information. The maximum experimental efficiencies used for each material are listed in Table III, Supporting Information.

error bar of the $\eta_{\Gamma,sq}$ limit, indicating that they all suffer from interface or device-level losses in state-of-the-art cells. Absorbers with higher cumulative development efforts such as CdTe, amorphous silicon (a-Si) and kesterites (CZTS, CZTSe, and ACZTSSe) tend to lie closer to their FOM-driven efficiency limit compared to less developed absorbers such as BiOI, Zn_3P_2 , and $Cu_2BaSn(S,Se)$ (CBTSSe). The record efficiency of kesterite absorbers has recently climbed to 14.9% after years of stagnation [12] and the Γ_{PV} value of the current state-of-the-art kesterite absorbers (0.15) implies an efficiency limit of about 22% without further bulk property improvement. Nevertheless, this FOM value is still lower than in the best Sn-based perovskites. These low-band gap perovskites have also experienced significant progress in both record efficiency and bulk material quality, with $CH_5N_2SnI_3$ (FASnI₃) now exhibiting a FOM of 0.25 and an efficiency limit of about 23%. Interestingly, two novel PV absorbers ($BaZrS_3$ and $BaCd_2P_2$) have already reached this intermediate FOM range despite their very short history and lack of functioning solar cells.

Some of the considered absorbers fall in the low FOM region ($\Gamma_{PV} < 0.001$). Among them, the record efficiency of $AgBiS_2$ seems difficult to increase without improving

the bulk properties of the absorber, a factor that may slow down the rapid progress $AgBiS_2$ solar cells have experienced in recent years. [13] The chemically related $NaBiS_2$ shows significantly less promise as a PV absorber due to its lower FOM. SnS has about the same FOM value as $NaBiS_2$ but it seems to already have reached its (low) efficiency limit, possibly due to its longer development history. The figure of merit of the recently proposed antiperovskite Ag_3SI is still so low ($< 10^{-7}$) that even a perfect device structure and perfect interfaces would not help this absorber reach meaningful efficiencies. SbSI lies in the inaccessible region (although within error bar of $\eta_{\Gamma,sq}$). This may partially be due to its mesoporous cell architecture, for which the $\eta_{\Gamma,sq}$ efficiency limit does not strictly apply. [1]

The combination of experimental record efficiencies $\eta_{exp,sq}$ and the Γ_{PV} figure of merit enables researchers to quantify the relative urgency of device-level optimization and bulk absorber-level optimization for a given single-junction PV technology. In Fig. 3, a device quality factor defined as $\eta_{exp,sq}/\eta_{\Gamma,sq}$ is plotted against an absorber quality factor simply defined as $\eta_{\Gamma,sq}$. For some PV technologies (e.g., BiOI, Zn_3P_2 , CBTSSe, $BaZrS_3$, $BaCd_2P_2$) the absorber quality factor is substantially higher than

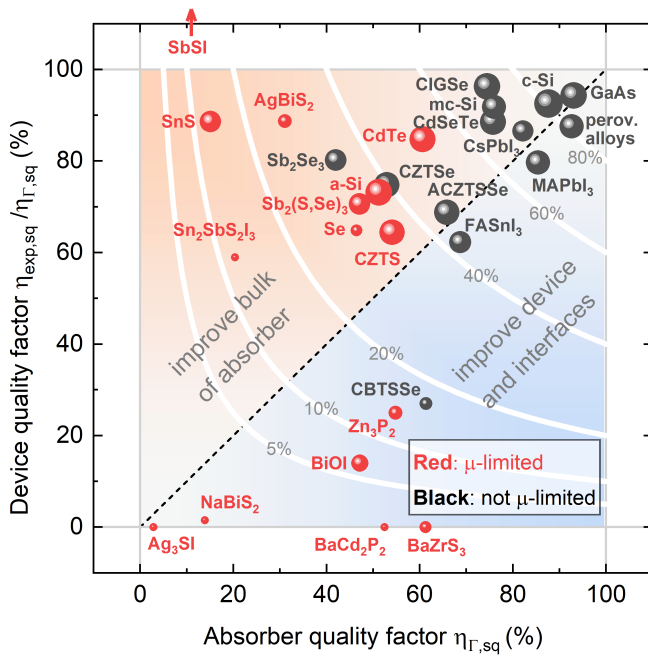


FIG. 3. Quantification of the current quality of 28 PV absorbers at the device/interface level (y-axis) and at the bulk absorber property level (x-axis). Along the dashed line the device quality factor is equal to the absorber quality factor. For materials located above this line, improving the bulk properties of the absorber is likely more urgent than improving the device structure, interfaces, contact/transport layers in their solar cells. For materials located below the dashed line, absorber development is likely less urgent. The white contour lines indicate device/absorber quality factor combinations with a constant $\eta_{\text{exp,sq}}$ efficiency limit (labeled as fraction of the SQ limit). Red data points indicate materials that would have a $> 10\%$ (relative) higher efficiency limit if their carrier mobility could be increased from their current experimental value to infinity. The other materials (black points) would benefit less from a mobility increase.

the device quality factor. In these cases, optimization of device structure, interfaces, contact and/or transport layers is arguably more urgent than improvement of the bulk properties of the absorber. For other technologies (e.g., CIGSe, SnS, AgBiS₂, SbSI) the device quality factor is close to 100% and improving the absorber quality seems to be the only realistic way to significantly improve their current record efficiency. By changing the μ values of the different PV materials (with everything else fixed) and applying Eqs. 2, 3, it is possible to determine which PV materials are limited by low carrier mobilities. It turns out that over half of the materials shown in Figs. 2, 3 would have an efficiency limit higher by at least 10% relative if their carrier mobilities could be increased to infinity. These are examples of PV materials for which the classic detailed balance analysis would overestimate efficiency limits.

A key question that naturally arises at this point is whether it is actually possible to improve the bulk prop-

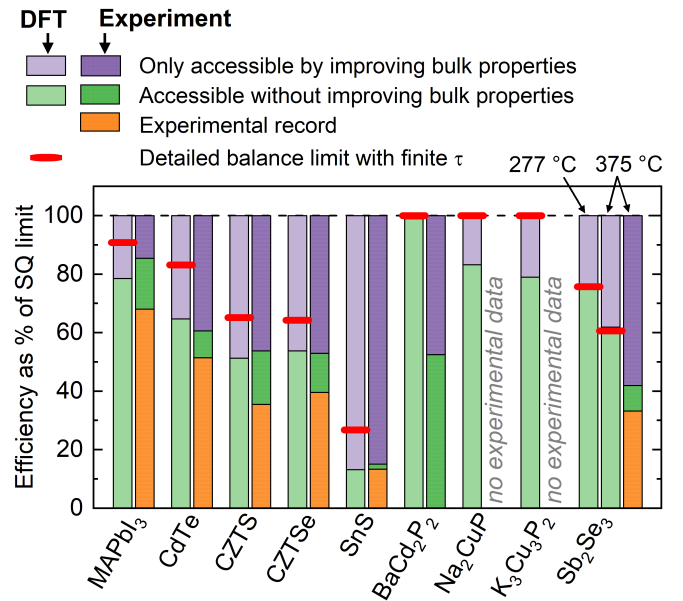


FIG. 4. Maximum efficiencies achievable by 9 PV absorbers, according to the Γ_{PV} FOM using DFT-calculated properties (pale colors) and experimentally measured properties on state-of-the-art specimens (bright colors). These efficiency limits are compared to classic detailed-balance efficiency limits including non-radiative recombination (but not considering finite values of μ , n , and ϵ). The top of the green bars corresponds to the $\eta_{\Gamma,\text{sq}}$ limit. The top of the orange bars is the current record efficiency. The purple bars represent the gap in efficiency between the $\eta_{\Gamma,\text{sq}}$ limit and the SQ limit. The material properties used to obtain Γ_{PV} from DFT modeling are listed in Table II, Supporting Information.

erties of a given absorber beyond its current state of the art. For example, is there any hope of developing SnS beyond its modest 18% absorber quality factor? Could we have foreseen the significant recent FOM increase of kesterite absorbers? Can perovskite absorbers become even better? To search for answers, we can turn to first-principles calculations of material properties. Until recently, only six out of the eight bulk properties necessary to calculate the FOM (α , σ , n , ϵ , m , E_g) were within reasonable reach of materials modeling methods based on density functional theory (DFT). However, recent methodological advances [14, 15] now allow computational scientists to also estimate τ by calculating carrier capture coefficients of point defects, [16] as well as μ by more efficient calculation of carrier scattering rates. [17]

Hence, it is also possible to calculate the Γ_{PV} FOM and the corresponding $\eta_{\Gamma,\text{sq}}$ efficiency limit using computationally-determined properties, even for the case of materials that have never been synthesized. Some examples are shown in Fig. 4. The DFT-derived $\eta_{\Gamma,\text{sq}}$ limits (pale colors) in materials with significant accumulated experience (MAPbI₃, CdTe, CZTS, CZTSe, SnS) are quite close to the corresponding limits derived from experimental properties (bright colors). This is a remark-

able finding, implying that the ultimate efficiency potential of these absorbers could have been quantitatively predicted with reasonable accuracy before commencing any experimental development work. Still, the experiment/computation agreement can sometimes be partially attributed to error cancellation. Furthermore, comparison of PV material properties from experiment and computation should always be done with an awareness of possible limitations. A discussion is given in the Supporting Information.

Two other results in Fig. 4 are worth noting. First, the very recently proposed BaCdP₂ [18] is the only absorber in Fig. 4 that may be able to reach the SQ limit according to the DFT-based Γ_{PV} FOM. The above-discussed good agreement between $\eta_{\Gamma,sq}$ values obtained on a computer and in the lab for more established absorbers gives credibility to this exciting finding. Second, efficiency limits calculated through the Γ_{PV} FOM can be compared to the corresponding limits calculated with current state-of-the-art detailed-balance methods including non-radiative recombination (finite τ) but no collection losses (infinite μ). [4–7] For DFT-modeled absorbers, these methods are often referred to as the spectroscopically limited maximum efficiency (SLME) following the treatment in Ref. [4]. As expected, the inductive $\eta_{\Gamma,sq}$ efficiency limit is tighter than the deductive SLME limit due to the explicit inclusion of μ , n , and ϵ .

Another interesting application of the Γ_{PV} FOM is tracking the progress of different PV absorbers and their record solar cells through history. These timelines are plotted in Fig. 5 for four PV absorber types and can be related to technological breakthroughs in absorber processing and to device structure/interface innovations. As an example, let us follow the history of CIGSe. Record CIGSe cells between 1985 and 1996 were operating at the maximum efficiency allowed by the absorber’s bulk quality at that time. During this period, the FOM of CIGSe improved due to increases in τ and n following the introduction of a Cu-rich growth phase, as well as Na and Ga incorporation. [19] Steady improvements to the three-stage evaporation process in CIGSe over the next decade [19] resulted in significantly longer carrier lifetimes and a large increase in the Γ_{PV} FOM. However, the device quality as of 2009 was no longer sufficient for CIGSe cells to achieve their full potential. The main breakthrough allowing CIGSe solar cells to again approach their $\eta_{\Gamma,sq}$ efficiency limit in the 2020’s was the introduction of an alkali post-deposition treatment (2013) to improve the charge-separating heterointerface. [20]

In conclusion, the Γ_{PV} FOM can be considered a generalization of previously proposed $\alpha\tau$ and $\alpha\tau\mu$ FOMs. It seems to be applicable across a wide range of realistic combinations of bulk properties of possible PV absorber materials (Fig. 1). The efficiency limit η_{Γ} set by the Γ_{PV} FOM is more stringent than the corresponding limit set by deductive methods based on the principle of detailed balance. The main reason is that efficiency losses by imperfect carrier collection (primarily influencing J_{sc} and

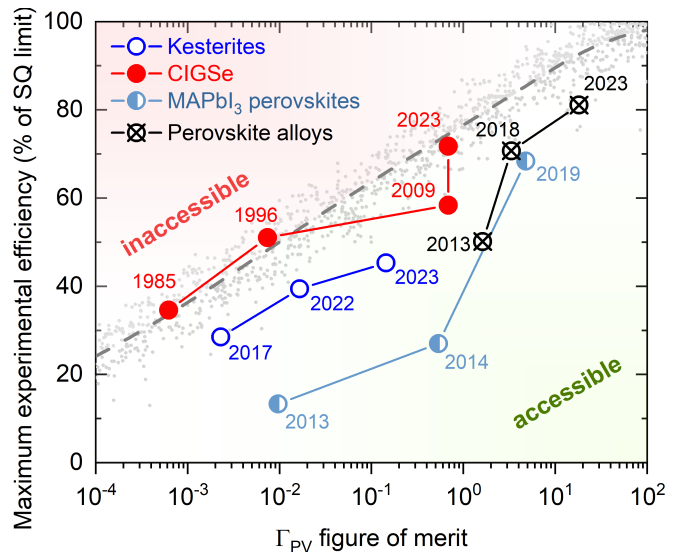


FIG. 5. Development history of four classes of PV absorbers. Kesterites include absorbers with the general $(Ag,Cu)_2ZnSn(S,Se)_4$ formula; CIGSe stands for $Cu(In,Ga)Se_2$; MAPbI₃ perovskites only include materials without alloying. Perovskite alloys are absorbers with the general $(MA,FA,Cs)Pb(I,Br,Cl)_3$ formula. Numbers next to each data point refer to the year of publication. The dashed line is the $\eta_{\Gamma,sq}$ efficiency limit (Eq. 3, same as in Fig. 2). The small grey data points are the training set used to derive the Γ_{PV} FOM and giving an impression of the error bar of the $\eta_{\Gamma,sq}$. Raw data is listed in Tables IV–VI, Supporting Information.

FF) are taken into account in Γ_{PV} by including the carrier mobility, doping density, and dielectric constant of the PV absorber as relevant properties. Applying the Γ_{PV} FOM to 28 established and emerging PV materials (Fig. 2) allows us to quantitatively visualize their current development status, to decide whether to prioritize bulk absorber improvement or device-level improvement (Fig. 3), and to track the impact of different innovations in absorber processing versus device/interface processing and design (Fig. 5). With some caveats, the η_{Γ} efficiency limit obtained using DFT-calculated properties seems to be an acceptable descriptor of the ultimate performance level that may be expected from candidate PV absorbers (Fig. 4). This gives credibility to computational screening workflows that include calculation of the eight properties necessary to evaluate the Γ_{PV} FOM. Intriguingly, some exotic phosphide compounds recently identified via such methods exhibit higher efficiency potential than many established PV absorbers.

ACKNOWLEDGEMENTS

This work was co-funded by the European Union (ERC, IDOL, 101040153). Views and opinions expressed are however those of the author only and do not necessar-

ily reflect those of the European Union or the European Research Council. Neither the European Union nor the

granting authority can be held responsible for them. This work was supported in part by a research grant (42140) from VILLUM FONDEN.

-
- [1] A. Crovetto, A phenomenological figure of merit for photovoltaic materials, *Journal of Physics: Energy* **6**, 025009 (2024).
- [2] W. Shockley and H. J. Queisser, Detailed Balance Limit of Efficiency of p-n Junction Solar Cells, *Journal of Applied Physics* **32**, 510 (1961).
- [3] J.-F. Guillemoles, T. Kirchartz, D. Cahen, and U. Rau, Guide for the perplexed to the Shockley–Queisser model for solar cells, *Nature Photonics* **13**, 501 (2019).
- [4] L. Yu and A. Zunger, Identification of Potential Photovoltaic Absorbers Based on First-Principles Spectroscopic Screening of Materials, *Physical Review Letters* **108**, 068701 (2012).
- [5] B. Blank, T. Kirchartz, S. Lany, and U. Rau, Selection Metric for Photovoltaic Materials Screening Based on Detailed-Balance Analysis, *Physical Review Applied* **8**, 024032 (2017).
- [6] T. Kirchartz and U. Rau, What Makes a Good Solar Cell?, *Advanced Energy Materials* **8**, 1703385 (2018).
- [7] S. Kim and A. Walsh, Ab initio calculation of the detailed balance limit to the photovoltaic efficiency of single p-n junction kesterite solar cells, *Applied Physics Letters* **118**, 243905 (2021).
- [8] J. Mattheis, U. Rau, and J. H. Werner, Light absorption and emission in semiconductors with band gap fluctuations—A study on Cu(In,Ga)Se₂ thin films, *Journal of Applied Physics* **101**, 113519 (2007).
- [9] T. Kirchartz, J. Mattheis, and U. Rau, Detailed balance theory of excitonic and bulk heterojunction solar cells, *Physical Review B* **78**, 235320 (2008).
- [10] P. Kaienburg, L. Krückemeier, D. Lübke, J. Nelson, U. Rau, and T. Kirchartz, How solar cell efficiency is governed by the $\alpha\mu\tau$ product, *Physical Review Research* **2**, 023109 (2020).
- [11] A. Richter, M. Hermle, and S. W. Glunz, Reassessment of the Limiting Efficiency for Crystalline Silicon Solar Cells, *IEEE Journal of Photovoltaics* **3**, 1184 (2013).
- [12] M. A. Green, E. D. Dunlop, M. Yoshita, N. Kopidakis, K. Bothe, G. Siefert, and X. Hao, Solar cell efficiency tables (Version 63), *Progress in Photovoltaics: Research and Applications* **32**, 3 (2024).
- [13] Y. Wang, S. R. Kavanagh, I. Burgués-Ceballos, A. Walsh, D. Scanlon, and G. Konstantatos, Cation disorder engineering yields AgBiS₂ nanocrystals with enhanced optical absorption for efficient ultrathin solar cells, *Nature Photonics* **16**, 235 (2022).
- [14] A. M. Ganose, J. Park, A. Faghaninia, R. Woods-Robinson, K. A. Persson, and A. Jain, Efficient calculation of carrier scattering rates from first principles, *Nature Communications* **12**, 2222 (2021).
- [15] A. Alkauskas, Q. Yan, and C. G. Van de Walle, First-principles theory of nonradiative carrier capture via multiphonon emission, *Physical Review B* **90**, 075202 (2014).
- [16] S. Kim, J. A. Márquez, T. Unold, and A. Walsh, Upper limit to the photovoltaic efficiency of imperfect crystals from first principles, *Energy Environ. Sci.* **13**, 1481 (2020).
- [17] D. Dahliah, G. Brunin, J. George, V.-A. Ha, G.-M. Rignanese, and G. Hautier, High-throughput computational search for high carrier lifetime, defect-tolerant solar absorbers, *Energy Environ. Sci.* **14**, 5057 (2021).
- [18] Z. Yuan, D. Dahliah, M. R. Hasan, G. Kassa, A. Pike, S. Quadir, R. Claes, C. Chandler, Y. Xiong, V. Kyveryga, P. Yox, G.-M. Rignanese, I. Dabo, A. Zakutayev, D. P. Fenning, O. G. Reid, S. Bauers, J. Liu, K. Kovnir, and G. Hautier, Discovery of the Zintl-phosphide BaCd₂P₂ as a long carrier lifetime and stable solar absorber, *Joule* **10.1016/j.joule.2024.02.017** (2024).
- [19] R. Scheer and H.-W. Schock, *Chalcogenide Photovoltaics* (Wiley-VCH Verlag, Weinheim, Germany, 2011).
- [20] A. Chirilă, P. Reinhard, F. Pianezzi, P. Bloesch, A. R. Uhl, C. Fella, L. Kranz, D. Keller, C. Gretener, H. Hagerdorfer, D. Jaeger, R. Erni, S. Nishiwaki, S. Buecheler, and A. N. Tiwari, Potassium-induced surface modification of Cu(In,Ga)Se₂ thin films for high-efficiency solar cells, *Nature Materials* **12**, 1107 (2013).